Expanded View Figures

Figure EV1. Immunofluorescence and electron microscopic analyses of *Gtsf1*-deficient testes (related to Fig 1).

A Elevated expression of LINE-1 and IAP in early postnatal periods caused by *Gtsf1* deficiency. Immunostaining of *Gtsf1*$^{+/-}$ and *Gtsf1*$^{-/-}$ testes at postnatal days 0, 4, and 8 with antibody to Line-1 ORF1 protein (left panel, green) and IAP GAG protein (right panel, green). DNA was stained with DAPI (red). Scale bar, 10 μm.

B Expression of GTSF1 in early postnatal periods. Immunostaining of *Gtsf1*$^{+/-}$ and *Gtsf1*$^{-/-}$ testes at postnatal days 0, 4, and 8 with antibody to GTSF1 (green). DNA was stained with DAPI (red). Scale bar, 10 μm.

C Histological analysis of *Gtsf1*-deficiency phenotypes. Immunostaining of *Gtsf1*$^{+/-}$ and *Gtsf1*$^{-/-}$ E17.5 testes with anti-DNMT3A2 (upper panel, green) and anti-DNMT3L (lower panel, green) antibodies. DNA was stained with DAPI (red). Localization of DNMT3L and DNMT3A/3A2 was unaffected in the prenatal *Gtsf1*$^{-/-}$ testes. Scale bar, 10 μm.

D Electron microscopy of *Gtsf1*$^{+/-}$ (upper panel) and *Gtsf1*$^{-/-}$ (lower panel) E17.5 prospermatogonia. Right panels (scale bar, 1 μm) are magnified views of the boxed region in the left panels (scale bar, 5 μm). Arrows indicate intermitochondrial cement.

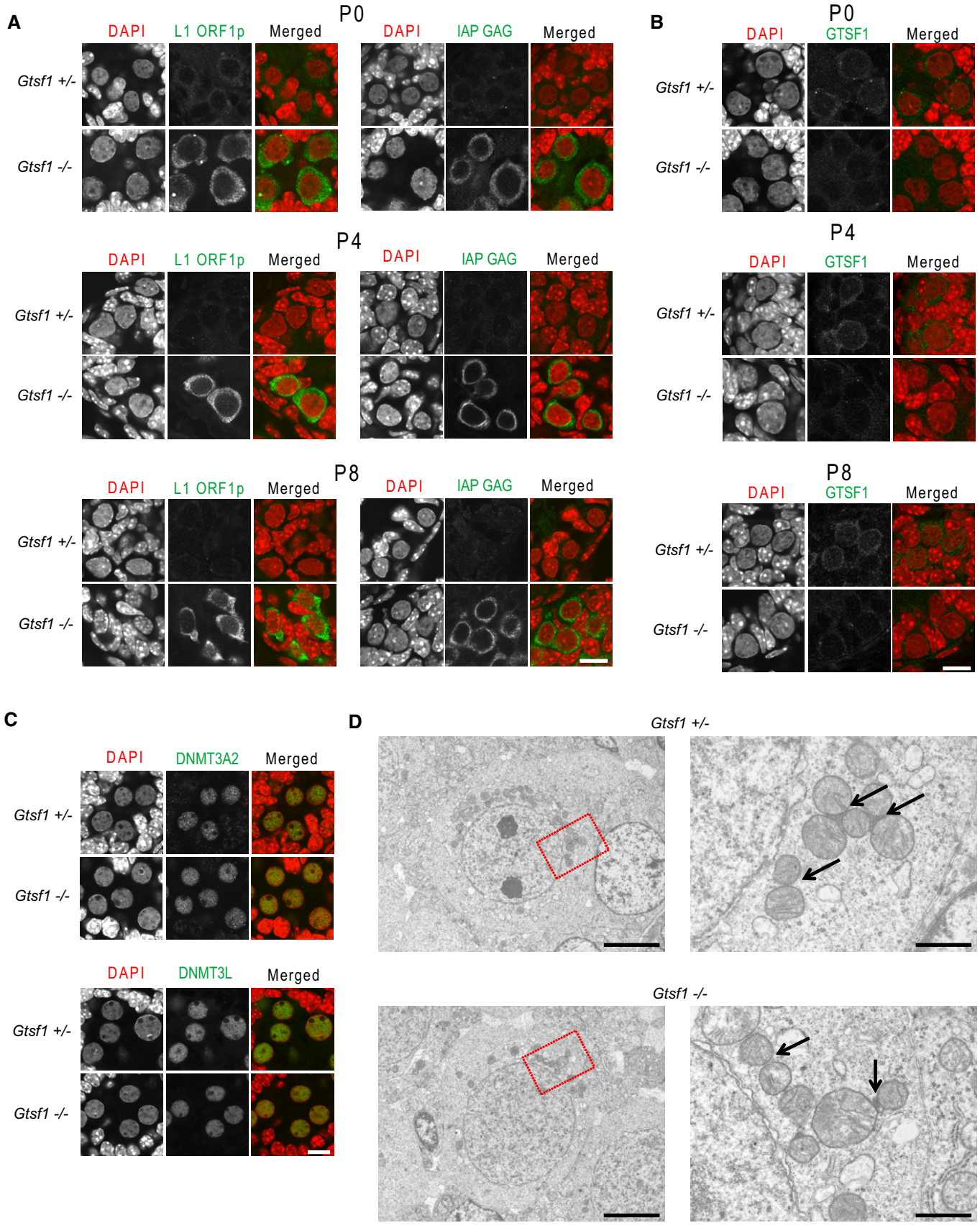
A
P0
DAPI
L1 ORF1p
Merged
DAPI
IAP GAG
Merged
Gtsf1 +/-
Gtsf1 -/-
P4
P8
B
DAPI
GTSF1
Merged
C
DAPI
DNMT3A2
Merged
DAPI
DNMT3L
Merged
D
Gtsf1 +/-
Gtsf1 -/-

Figure EV1.

Figure EV2. Analysis of GTSF1-associated proteins (related to Fig 2).

A GST pull-down analysis of the interaction of GTSF1 with MILI, MIWI, TDRD1, or TDRD9. The GST-fusion proteins bound to glutathione sepharose were incubated with adult testis lysates. In some experiments, testis lysates were pretreated with RNase A prior to incubation with GST-fusion proteins. The proteins bound to GST-fusion proteins were analyzed by SDS–PAGE followed by Western blotting with antibodies to MILI, MIWI, TDRD1, and TDRD9 (upper panels). CBB staining shows the amount of the GST-fusion proteins in each of the reactions (lower panels).

B Schematic illustration of mouse GTSF1 protein. Amino acid sequences in the central regions of five species, including mouse, are shown. Black-and-white inverted characters represent conserved aromatic amino acid residues in the central regions among the species, which were used for alanine substitutions in pull-down analysis. These aromatic amino acid residues are surrounded by several negatively charged amino acid residues (in blue font).

C GST pull-down analysis of the interaction of mutated CR proteins with MILI or MIWI complexes. The GST-fusion proteins bound to glutathione sepharose were incubated with adult testis lysates. The proteins bound to GST-fusion proteins were analyzed by SDS–PAGE followed by Western blotting with antibodies to MILI and MIWI (upper panels). CBB staining shows the amount of the GST-fusion proteins in each of the reactions (lower panels).

D Immunoprecipitation analysis of the binding of GTSF1 to several piRNA pathway components. Myc-tagged GTSF1 was co-expressed with FLAG-tagged MAEL, MILI, MIWI, MIWI2, MVH, or His-tagged TDRD1 in HEK293 cells. Lysates of the transfected cells were immunoprecipitated with an anti-Myc antibody and separated by SDS–PAGE, followed by Western blotting using the indicated antibodies.

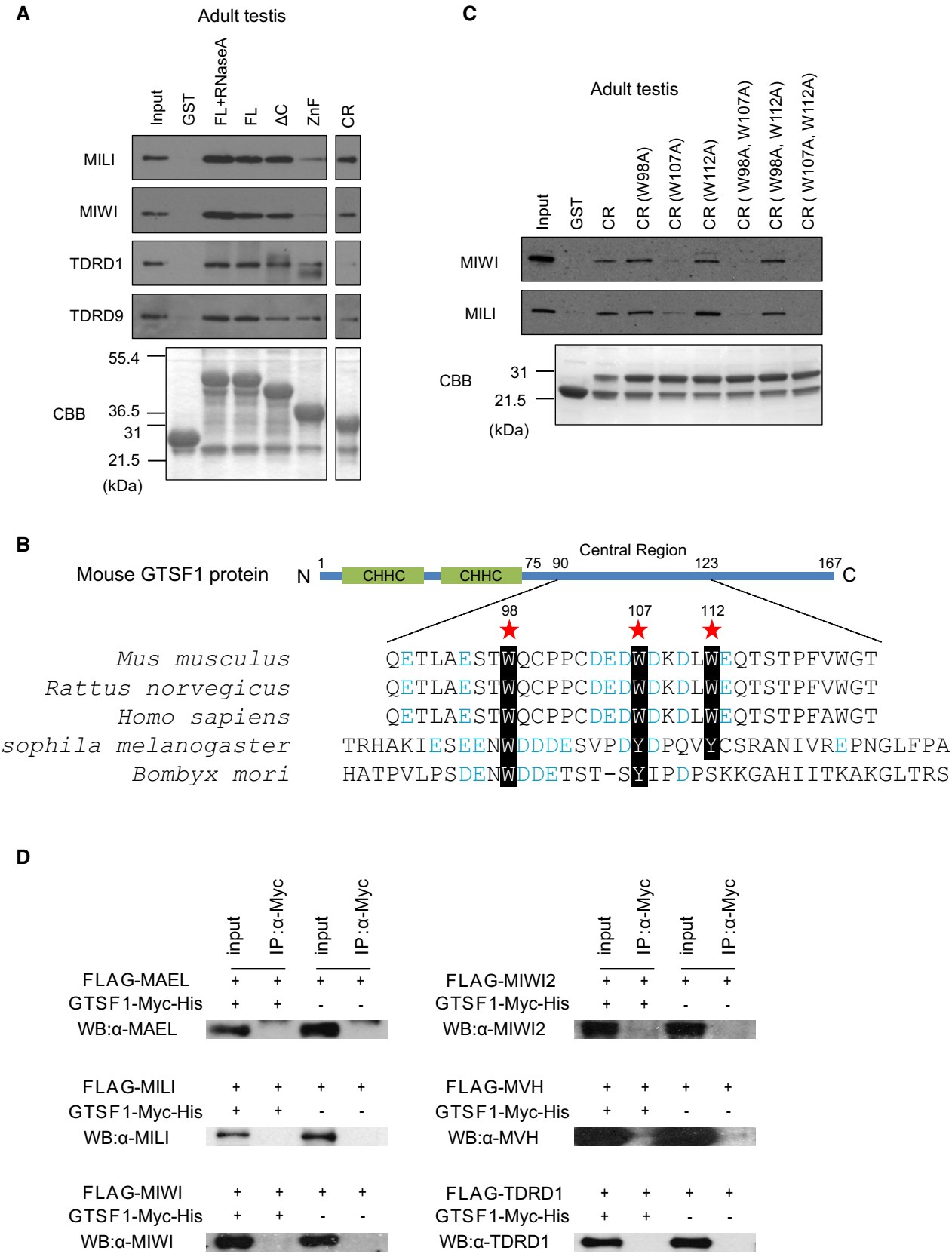

Figure EV2.

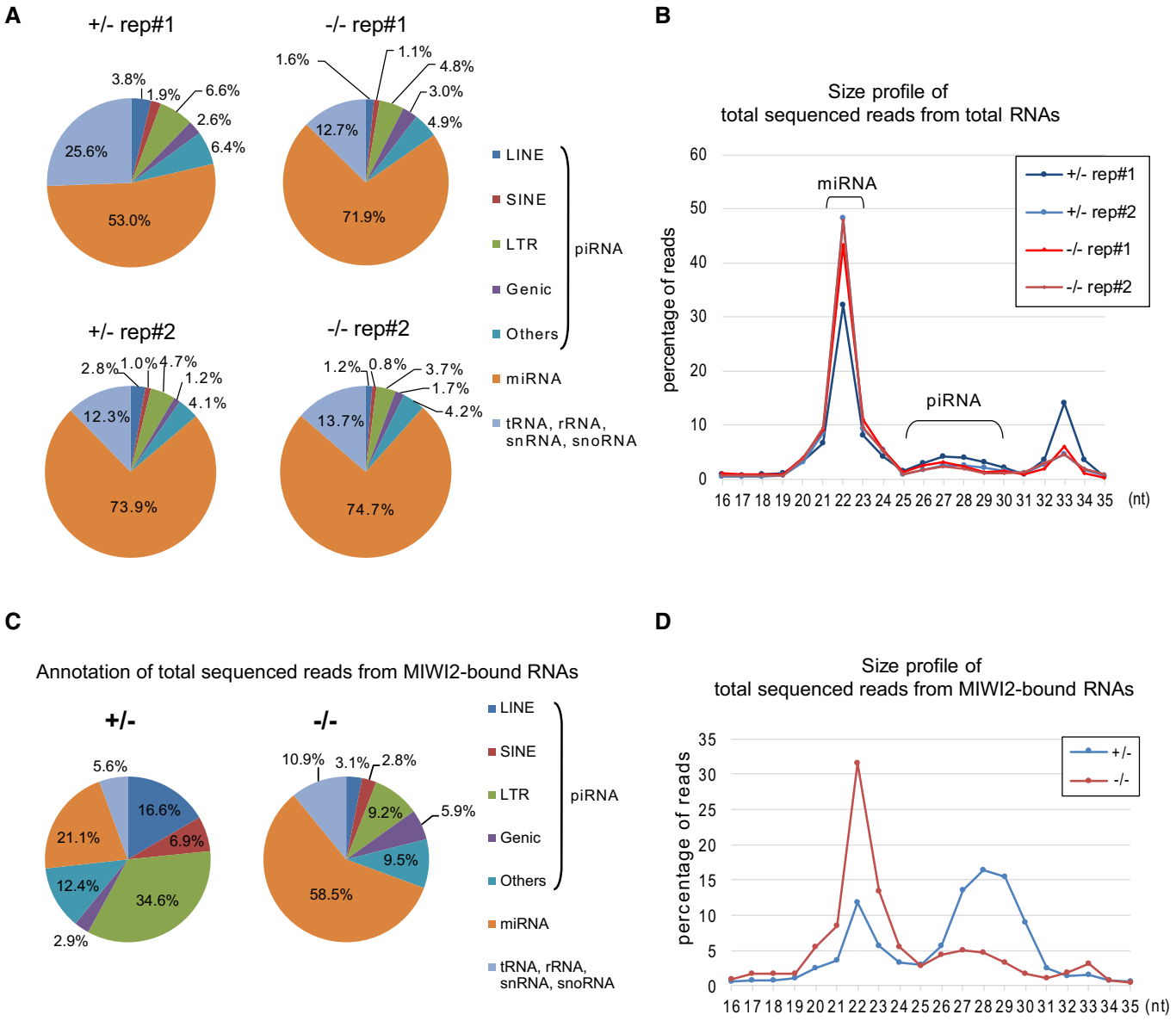

Figure EV3. Analysis of deep-sequencing data obtained from the libraries of total small RNAs and MIWI2-bound piRNAs (related to Fig 3).

A RNA annotation of total sequenced reads from total RNA libraries prepared from *Gtsf1*$^{+/-}$ and *Gtsf1*$^{-/-}$ E17.5 testes (n = 2).

B Size profile of total sequenced reads from total RNA libraries prepared from *Gtsf1*$^{+/-}$ and *Gtsf1*$^{-/-}$ E17.5 testes (n = 2). Shown is the percentage of total reads of each length to total reads of 16–35 nt RNAs.

C RNA annotation of total sequenced reads from MIWI2-bound RNA libraries prepared from *Gtsf1*$^{+/-}$ and *Gtsf1*$^{-/-}$ E17.5 testes.

D Size profile of total sequenced reads from MIWI2-bound RNA libraries prepared from *Gtsf1*$^{+/-}$ and *Gtsf1*$^{-/-}$ E17.5 testes. Shown is the percentage of total reads of each length in total reads of 16–35 nt MIWI2-bound RNAs.

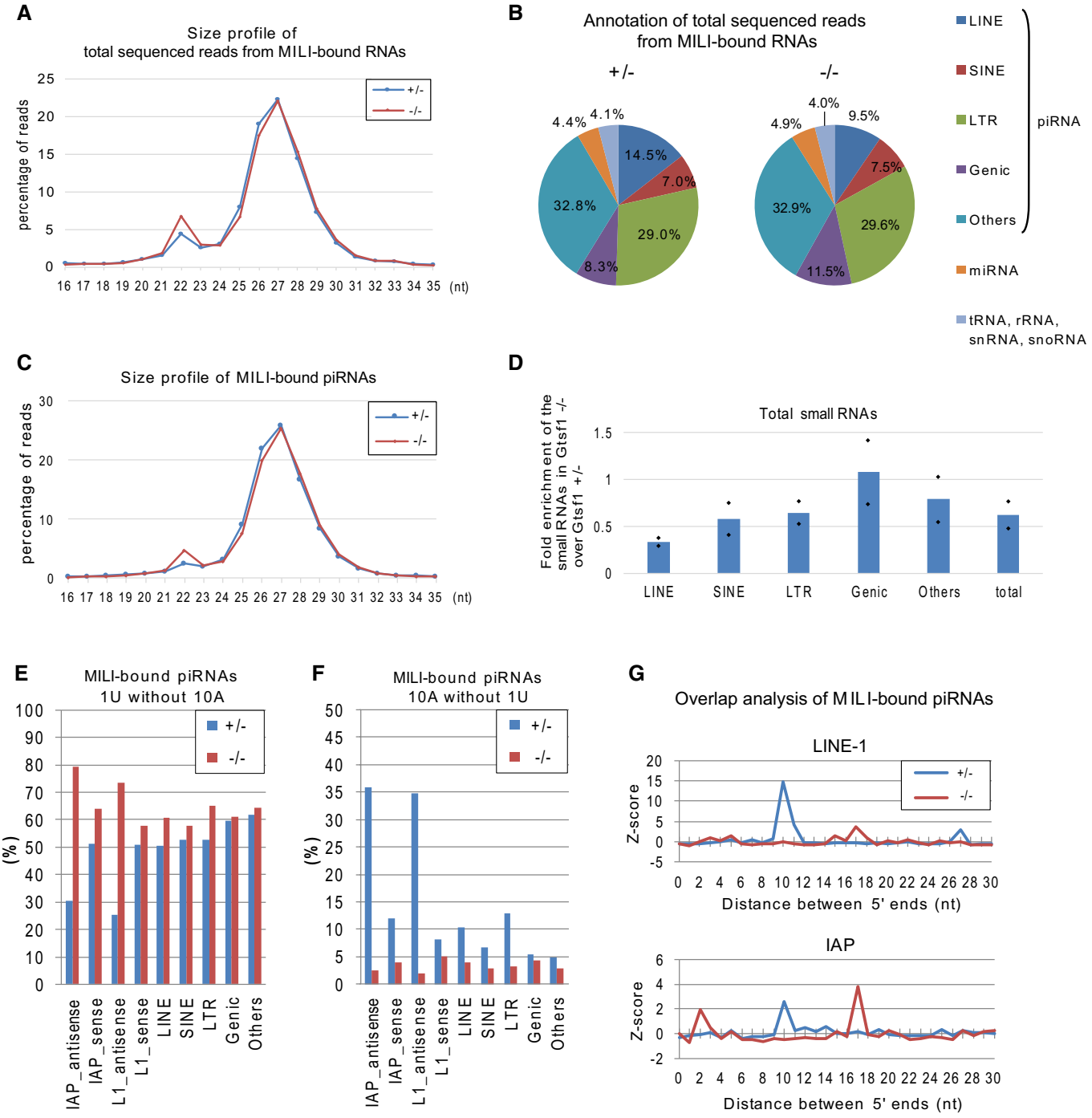
A
Size profile of
total sequenced reads from MILI-bound RNAs
percentage of reads
+/-
-/-
(nt)
B
Annotation of total sequenced reads
from MILI-bound RNAs
+/-
-/-
4.4%
4.1%
14.5%
7.0%
32.8%
29.0%
8.3%
4.9%
4.0%
9.5%
7.5%
32.9%
29.6%
11.5%
LINE
SINE
LTR
Genic
Others
piRNA
miRNA
tRNA, rRNA,
snRNA, snoRNA
C
Size profile of MILI-bound piRNAs
percentage of reads
+/-
-/-
(nt)
D
Total small RNAs
Fold enrichment of the
small RNAs in Gtsf1 -/-
over Gtsf1 +/-
LINE
SINE
LTR
Genic
Others
total
E
MILI-bound piRNAs
1U without 10A
(%)
+/-
-/-
IAP_antisense
IAP_sense
L1_antisense
L1_sense
LINE
SINE
LTR
Genic
Others
F
MILI-bound piRNAs
10A without 1U
(%)
+/-
-/-
IAP_antisense
IAP_sense
L1_antisense
L1_sense
LINE
SINE
LTR
Genic
Others
G
Overlap analysis of MILI-bound piRNAs
LINE-1
Z-score
+/-
-/-
Distance between 5' ends (nt)
IAP
Z-score
Distance between 5' ends (nt)

Figure EV4.

Figure EV4. Analysis of deep-sequencing data obtained from the libraries of MILI-bound piRNAs and total small RNAs (related to Fig 4).

A Size profile of total sequenced reads from MILI-bound RNA libraries prepared from *Gtsf1*$^{+/-}$ and *Gtsf1*$^{-/-}$ E17.5 testes. Shown is the percentage of MILI-bound small RNA reads of each length in total reads of 16–35 nt MILI-bound RNAs.

B RNA annotation of total sequenced reads from MILI-bound RNA libraries prepared from *Gtsf1*$^{+/-}$ and *Gtsf1*$^{-/-}$ E17.5 testes.

C Size profile of the piRNAs in MILI-bound RNA libraries prepared from *Gtsf1*$^{+/-}$ and *Gtsf1*$^{-/-}$ E17.5 testes. Shown is the percentage of MILI-bound piRNA reads of each length in the total reads of 16–35 nt MILI-bound piRNAs.

D Small RNAs are less abundant in *Gtsf1*$^{-/-}$ total small RNA libraries. Shown is the fold enrichment of each annotated piRNA in *Gtsf1*$^{-/-}$ over *Gtsf1*$^{+/-}$. Total read number of each annotated piRNA was normalized to that of 22 nt miRNA in the same libraries and plotted relative to its average value in *Gtsf1*$^{+/-}$ testes. Bar graphs represent the mean of two biological replicates in each annotated piRNA.

E The 1U signature for primary processing was increased in transposon-derived piRNAs in the *Gtsf1* mutant. Shown is the percentage of small RNAs containing 1U without 10A in each annotated group of MILI-bound piRNAs from *Gtsf1*$^{+/-}$ and *Gtsf1*$^{-/-}$ E17.5 testes.

F The 10A ping-pong signature was lost in transposon-derived piRNAs under *Gtsf1* deficiency. Shown is the percentage of small RNAs containing 10A without 1U in each annotated group of MILI-bound piRNAs from *Gtsf1*$^{+/-}$ and *Gtsf1*$^{-/-}$ E17.5 testes.

G Ping-pong *Z*-scores [47] for the significance of the distance between the 5′ ends of complementary MILI-bound piRNAs for LINE-1 (upper panel) and IAP (lower panel) from the *Gtsf1*$^{-/-}$ and *Gtsf1*$^{+/-}$ E17.5 testes.

Figure EV5. Mapping of small RNAs to LINE-1 sequence (related to Figs 3 and 4).

A–H Mapping of small RNAs derived from *Gtsf1*$^{+/-}$ (A, C, E, and G) and *Gtsf1*$^{-/-}$ (B, D, F, and H) testes to the genomic sequences of LINE-1 (Accession No. M13002), allowing up to three mismatches. The piRNAs for IAP from MILI-bound (A, B), MIWI2-bound (C, D), and two replicates of total (E–H) small RNA libraries were subjected to the analysis. The *x*-axis shows the position in M13002 sequence. The *y*-axis shows the normalized read count relative to 22 nt miRNAs in the deep-sequencing data from each library. Sense and antisense reads to retrotransposon transcripts are shown in blue and orange, respectively.

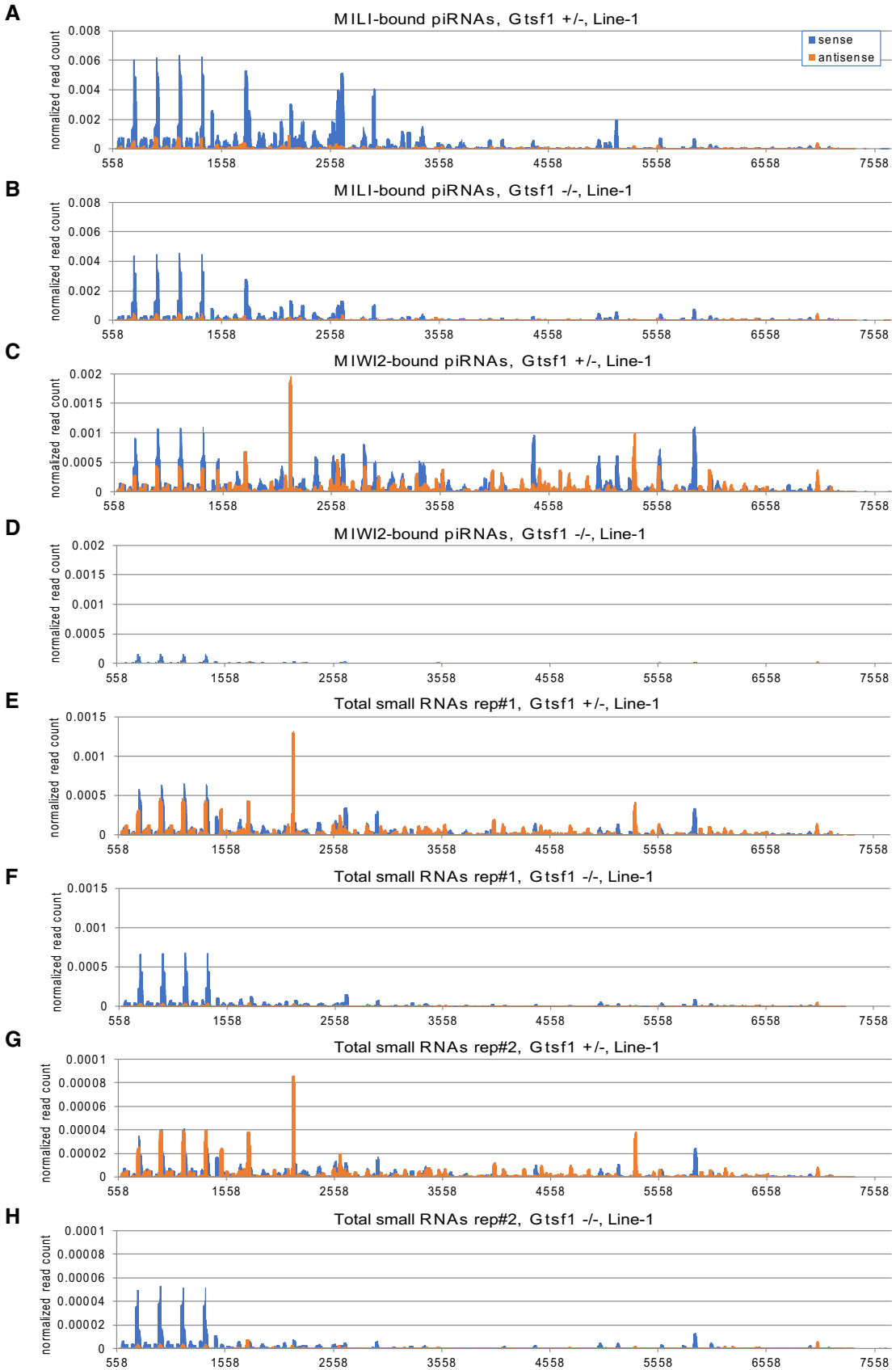
A
MILI-bound piRNAs, Gtsf1 +/-, Line-1
sense
antisense
normalized read count
0.008
0.006
0.004
0.002
0
558
1558
2558
3558
4558
5558
6558
7558
B
MILI-bound piRNAs, Gtsf1 -/-, Line-1
C
MIWI2-bound piRNAs, Gtsf1 +/-, Line-1
0.002
0.0015
0.001
0.0005
D
MIWI2-bound piRNAs, Gtsf1 -/-, Line-1
E
Total small RNAs rep#1, Gtsf1 +/-, Line-1
F
Total small RNAs rep#1, Gtsf1 -/-, Line-1
G
Total small RNAs rep#2, Gtsf1 +/-, Line-1
0.0001
0.00008
0.00006
0.00004
0.00002
H
Total small RNAs rep#2, Gtsf1 -/-, Line-1

Figure EV5.

Figure EV6. Mapping of small RNAs to IAP sequence (related to Figs 3 and 4).

A–H Mapping of piRNAs derived from *Gtsf1*$^{+/-}$ (A, C, E, and G) and *Gtsf1*$^{-/-}$ (B, D, F, and H) testes to the genomic sequences of IAP (Accession No. M17551), allowing up to three mismatches. The piRNAs for IAP from MILI-bound (A, B), MIWI2-bound (C, D), and two replicates of total (E–H) small RNA libraries were subjected to the analysis. The *x*-axis shows the position in M17551 sequence. The *y*-axis shows the normalized read count relative to 22 nt miRNAs in the deep-sequencing data from each library. Sense and antisense reads to retrotransposon transcripts are shown in blue and orange, respectively.

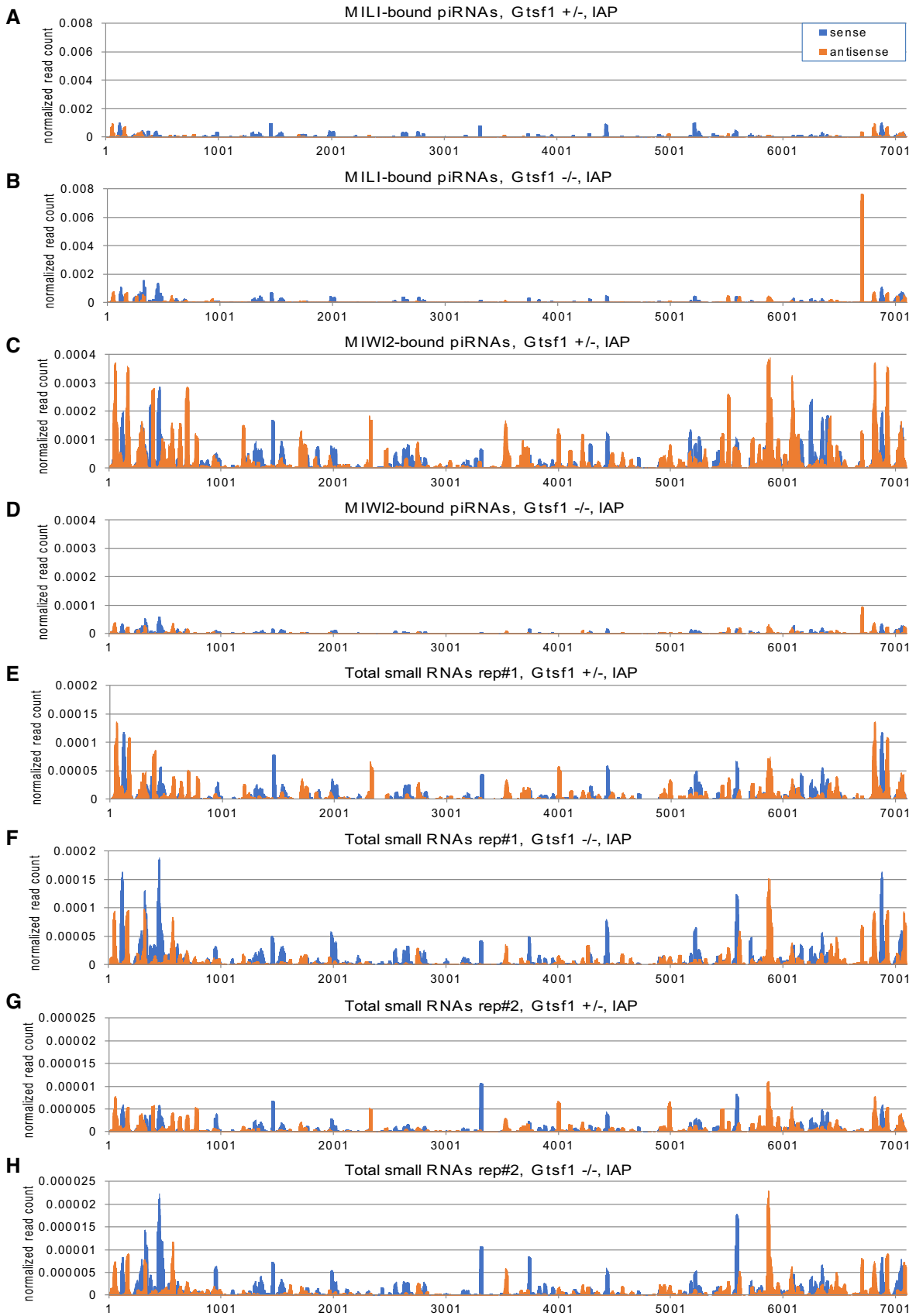

Figure EV6.